Biomechanical Study of the Resurfacing Hip Arthroplasty

Finite Element Analysis of the Femoral Component

Yuichi Watanabe, MD,* Naoto Shiba, MD,* Shigeaki Matsuo, BS,†
Fujio Higuchi, MD,* Yoshihiko Tagawa, PhD,† and Akio Inoue, MD*

Abstract: Finite element analysis was performed using 3-dimensional models to examine the biomechanical characteristics of the femoral component in resurfacing hip arthroplasty. Stress concentration was observed in the cortical bone adjacent to the rim of the prosthesis. Stress shielding was observed in the anterosuperior regions on the cancellous bone cross-sections near the cup rim. These biomechanical characteristics may lead to complications such as femoral neck fractures in patients with osteopenic bone and long-term loosening. **Key words:** finite element method, resurfacing hip arthroplasty, stress concentration, stress shielding, biomechanics.

Advantages of resurfacing hip arthroplasty compared with total hip arthroplasty include minimal bone resection, easier revision, and reduction in the stress shielding in the proximal femur [1]. The McMinn Resurfacing Hip Arthroplasty (Corin Medical Ltd, Cirencester, UK), which is a cemented metal-on-metal resurfacing arthroplasty, was performed in 11 cases of coxarthrosis at our institution. Three failures have occurred during the short-term follow-up among these 11 cases. Two patients sustained femoral neck fractures, and the other developed loosening in the acetabular component. One femoral neck fracture occurred just below the femoral component in a patient with adult-onset Still's disease. Our hypothesis was that this type of prosthesis was not appropriate for patients with brittle bone because of its biomechanical characteristics. Currently, there are relatively few biomechanical data on resurfacing hip arthroplasty compared with the larger body of research on conventional total hip arthroplasty. Understanding the precise biomechanical characteristics of these implants is important in their clinical application. The present study evaluated the biomechanical characteristics after resurfacing hip arthroplasty using finite element analysis (FEA) with 3-dimensional models.

*From the *Department of Orthopaedic Surgery, Kurume University School of Medicine; †Department of Mechanical Engineering, Kurume Institute of Technology, Kurume, Japan.*

Submitted December 14, 1998; accepted May 13, 1999.
No benefits or funds were received in support of this study.

Reprint requests: Yuichi Watanabe, MD, Department of Orthopaedic Surgery, Kurume University School of Medicine, 67 Asahi-machi, Kurume 830-0011, Japan.

doi:10.1054/arth.2000.1359
0883-5403/00/1504-0016$10.00/0

Materials and Methods

Finite Element Analysis

PRO/MECHANICA Structure Ver. 18.0 (Parametric Technology Corp, Waltham, MA), which is based on the p-version of the FEA, was used for this study. Three-dimensional models of the nonimplanted proximal femur and the proximal femur with resurfacing hip arthroplasty were employed for the FEA. These femoral models were established using the 3-dimensional digitizer, templates, and composite bone (Fig. 1) [2,3]. Three-dimensional finite element models of both models were automatically generated with 5-node tetrahedron elements. A

normal femur model consisted of 920 nodes and 1,725 elements, and a femur-implanted resurfacing hip arthroplasty model consisted of 1,348 nodes and 4,346 elements.

In this analysis, we applied the p-version of FEA, which was proposed by Szabo and Babuska [4]. It applies increasingly higher polynomial order to the displacement of each element edge. It continues to perform calculations and increase the polynomial order, until the convergence criteria are satisfied. Compared with conventional methods, it has the advantages of creating appropriate elements automatically, reducing the operation time, and enabling the accuracy to be monitored.

Loading Conditions (Boundary Conditions)

The femoral implant was fixed using bone–cement (polymethyl methacrylate [PMMA]). The loading conditions were applied using the technique developed by Davy and Kotzer et al. [5,6]. This method is the only one that generates precise loading on the hip joint using a sensorized prosthesis and can be used for FEA properly. The hip joint resultant forces for 3 different loading conditions during simulated ambulation with crutches were calculated. The first loading case (a joint resultant force of 1,320 N) represented the hip joint load at the first peak (P1) in the vertical component of the ground reaction force, the second loading case (a joint resultant force of 1,200 N) represented the hip joint load at the valley (V) in the vertical component of the ground reaction force, and the third loading case (a joint reaction force of 1,600 N) represented the hip joint load at the second peak (P2) in the vertical component of the ground reaction force (Table 1). With each case, the load was directed through the center of the femoral head. The magnitudes and vector forces of the gluteus maximus, gluteus medius, and gluteus minimus muscles were based on data from Crowninshield et al. [7] and Dostal and Andrews [8] (Table 1).

Table 1. Loading Condition of the Finite Element Analysis*

Gait Cycle	P1	V	P2
Load (N)	1,320	1,200	1,600
Gluteus maximus (N)	390	164.54	7.1
Gluteus medius (N)	354.55	818.19	602.55
Gluteus minimus (N)	35.45	109.1	10.64

Load on the hip joint using crutches and the magnitude of the muscle force in the gait cycle [5–8].

P1, first peak; V, valley; P2, second peak.

Material Property

Each element must be assigned the appropriate elastic constants of the material in the finite element model. Two material constants (elastic modulus and Poisson's ratio) were required. The elastic modulus was assumed for cortical bone (17,300 MPa), cancellous bone (1,000 MPa), cobalt-chrome alloy (200,000 MPa), and PMMA (2,000 MPa) [9]. Poisson's ratio was assumed for cortical bone (0.29), cancellous bone (0.29), cobalt-chrome alloy (0.3), and PMMA (0.19) [10]. It was assumed that the material connections were rigidly bonded.

Evaluation of Results

The stress distribution on cortical and cancellous bone was evaluated. For the evaluation of cancellous bone, 3 arbitrary cross-sectional areas vertical to the neck axis also were evaluated (Fig. 2). The first cross-sectional area was under the cup rim, the second on the distal femoral neck region, and the third around the tip of the peg. The stress and strain distribution were evaluated simultaneously.

Results

Cortical Bone Stress

Regardless of the changes in the loading conditions, resurfacing hip arthroplasty resulted in cortical bone stress concentration adjacent to the rim of the prosthesis, compared with the normal femur model (Fig. 3). The highest stress patterns were noted in the posteroinferior region near the rim of the prosthesis. Peak compressive stresses were 156 MPa at P1, 108.1 MPa at V, and 169.26 MPa at P2. In other areas, the stress values in the resurfacing hip arthroplasty model were negligibly different from those in the normal femur model.

Cancellous Bone Stress and Strain

First Cross-Section. The stress distribution on the first cross-sectional area of the resurfacing femur tended to decrease slightly in the anterosuperior region at P1 (Fig. 4A, bottom left; stress level, 0.231–0.489 MPa) compared with the normal femur (Fig. 4A, top left; stress level, >0.424 MPa). At V, it was less than that seen at P1 in the same region (Fig. 4A, bottom center; stress level, 0.231–0.489 MPa). This finding was considered a result of stress shielding. At P2, the stress tended to increase, so that there was a negligible difference between the normal femur and the resurfacing femur model (Fig. 4A, bottom right; stress level, >0.553 MPa).

The minimal principal strain distribution on the first cross-sectional area of the resurfacing femur

was similar to that of the stress distribution. The absolute values of the strain at P1 (Fig. 4B, bottom left; strain level, 69.6–467 μ strain) decreased in the anterosuperior region compared with the normal femur (Fig. 4B, top left; strain level, 334–533 μ strain). This tendency was slightly enhanced at V (Fig. 4B, bottom center; strain level, 69.6–467 μ strain) and was attenuated at P2 (Fig. 4B, bottom right; strain level, 69.6–401 μ strain).

Second Cross-Section. The stress distribution on the second cross-sectional area at P1, V, and P2 demonstrated increased stress concentration in the region inferior to the peg penetrating the surface of the cancellous bone P1 (Fig. 5A, bottom row; stress level, >0.489 MPa) compared with the normal femur (Fig. 5A, top row; stress level, 0.166–0.489 MPa). However, negligible differences in the change of color were noted between the models in the superior region of the second cross-sectioned area. (Fig. 5A). The absolute values of the strain on this surface increased in the region inferior to the hole at P1, V, and P2 (Fig. 5B, bottom row; strain level, >334 μ strain). The strain reflected the tendency of the stress distribution, which was consistent with compressive stress in the inferior region.

Third Cross-Section. The stress distribution on the third cross-sectional area demonstrated that stress concentrated around the tip of the peg for each gait cycle, with the highest levels at P2 (Fig. 6A, bottom right; stress level, >0.489 MPa). The absolute values of the minimal principal strain on the same cross-sectional area at P1 increased in the hole of the peg (Fig. 6B, bottom left; strain level, >334 μ strain). They also increased in the regions superior and inferior to the hole of the peg. This increase was consistent with compressive stress. Related phenomena occurred in this cross-sectional area at other points of the gait cycle. A large compressive strain was noted at P2 (Fig. 6B, bottom right; strain level, >334 μ strain).

Discussion

The resurfacing hip arthroplasty was developed from the original model of Smith-Petersen, which was termed the *mold arthroplasty* [11]. The original prosthesis had numerous problems. It required a precise surgical technique with a long period of rehabilitation postoperatively and an extended period of limited weight bearing. The long-term outcomes demonstrated a high revision rate [11].

Since then, several resurfacing hip arthroplasties have been developed and applied clinically. High failure rates have been reported by many surgeons, however, even with the alterations in materials and operative techniques. Howie et al. [12] reported that the rate of survival of 100 Wagner resurfacing hip arthroplasties was 40% at 8 years. Some hypotheses have been suggested to explain the cause of the failure, including excessive wear particles causing osteolysis at the interfaces, difficulty of the surgical technique, thinness of a polyethylene cup, disturbances in the vascularity under the metal head, and various biomechanical factors [12–17]. Most surgeons have abandoned the technique.

The McMinn resurfacing hip arthroplasty was developed in 1989 [1]. The expectation was that the failure rate for arthroplasties could be decreased by using a material other than polyethylene, which results in osteolysis. In addition, resurfacing hip arthroplasty maintains the femoral head and acetabular bone stock, avoids excessive production of wear debris by using metal-on-metal articulation, and avoids malpositioning of the femoral component [1]. Resurfacing hip arthroplasty with the metal-on-metal articulation is gradually experiencing a resurgence of popularity [1,18,19].

FEA has been performed to analyze the various total hip arthroplasties [1,9,14,16,17,20,21]. With respect to the resurfacing hip arthroplasty, unnatural stress shielding and stress concentration have been seen in the proximal femur [14,16,17,20]. Orr et al. [17], using 2-dimensional finite element models, reported that stress shielding occurred underneath the metal surface replacement cup, resulting in lower bone density in the femoral head, and that the addition of a central femoral cup fixation peg caused bone hypertrophy around the peg. De Waal Malefijt and Huiskes [14] found stress shielding in the proximal femur, depending on the interface condition, using 2-dimensional finite element models. The results of our study demonstrated stress shielding in the anterosuperior region of the femoral neck directly beneath the prosthesis and stress concentration around the peg in the inferior cross-section of the femoral neck at midstance. These findings were nearly consistent with those of Orr and De Waal Malefijt. Huiskes et al. [16] reported that the peak compressive stress occurred in the lateral cup region. Their model, however, did not take into account the anteversion of the proximal femur. The anatomic anteversion required to analyze the model accurately was incorporated in our study. Our results indicated that the peak compressive stress occurred in the posteroinferior cup-rim region. On the cortical bone stress distributions of the proximal femur (excluding the head-neck region), Shybut et al. [20] indicated that the presence of the surface replacement femoral component did not affect the stress and strain distribution in the femur. This tendency was also found in our analysis.

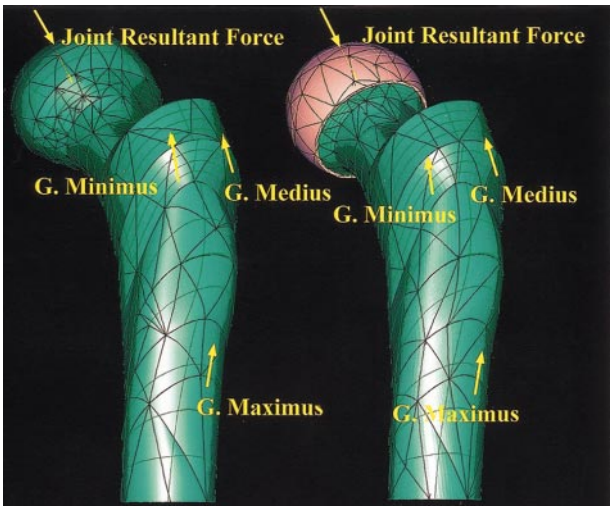

Fig. 1. Three-dimensional finite element models of a normal femur and a femur after resurfacing hip arthroplasty. G., gluteus.

In our study, the peak compressive cortical bone stress values around the cup rim with ambulation were high, with values almost reaching the ultimate strength of the femoral cortical bone, which was determined by mechanical experiments [22]. Because these were not *in vivo* experiments, the real ultimate strength of living cortical bone may be higher. The loading condition of the FEA in this study simulated ambulation using crutches, although the load without crutches is considered to be greater in routine activities of daily living. In our failed resurfacing hip arthroplasties, 1 patient with adult-onset Still's disease presented with a nontraumatic femoral neck fracture, which may have been secondary to osteopenia resulting from high-dose steroid use (Fig. 7). The fracture was observed at the femoral neck around the cup rim, in the region with the highest stress concentration on FEA. These results may indicate that this prosthesis should not be implanted in patients with osteopenic bone.

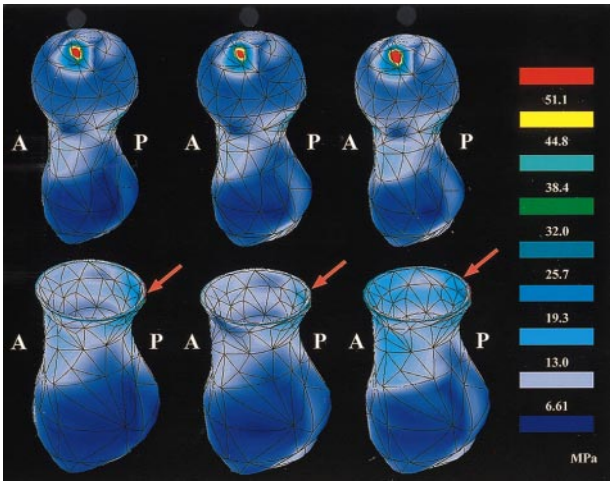

Fig. 3. The stress pattern (superior view) in the cortical bone of the proximal femur before (top row) and after (bottom row) implantation, represented by the Von Mises Stress (MPa) at first peak (P1; left column), valley (V; center column), and second peak (P2; right column). The stress was highest in the posteroinferior region of the prosthesis (arrow), with 156 MPa at the P1, 108.1 MPa at the V, and 169.26 MPa at the P2. A, anterior direction of these models; P, posterior direction of these models.

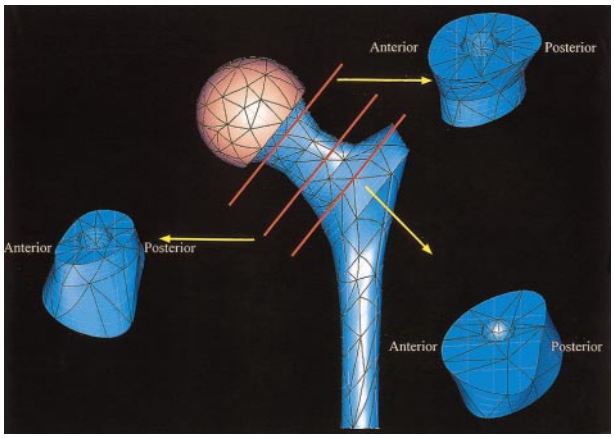

Fig. 2. Cross-sectional areas in the cancellous bone of the proximal femur with implantation. The cortical bone has been removed.

Stress shielding in resurfacing hip arthroplasty was reported by Philip et al. [23], who found completely or partially resorbed superior femoral bone heads in sheep with resurfacing hip arthroplasties. McMinn et al. [1] also reported that fractures in the femoral neck did not occur in all cases, although thinning in the femoral neck was found in some patients after the operation. Nordin et al. [24] showed that a reduction in the size of the bone diameter greatly decreased bone strength, especially in bending and with torsion. It was considered that some degree of thinning in the femoral neck might be caused by stress shielding and vascular damage to the proximal femur as the result of surgery. Because high stress shielding may lead to further failures, including fractures and loosening, it is not desirable.

With respect to the prosthetic stability, a resurfacing hip arthroplasty placed on cancellous bone may produce a less stable femoral component, compared with conventional femoral components. The femoral component of the conventional implanted femur model is inserted and covered with cortical bone, which has a mechanical property much stiffer than that of the cancellous bone. The FEA was useful in clarifying the biomechanical characteristics of the resurfacing hip arthroplasty. Further investigations are required to improve the resurfacing hip arthroplasty.

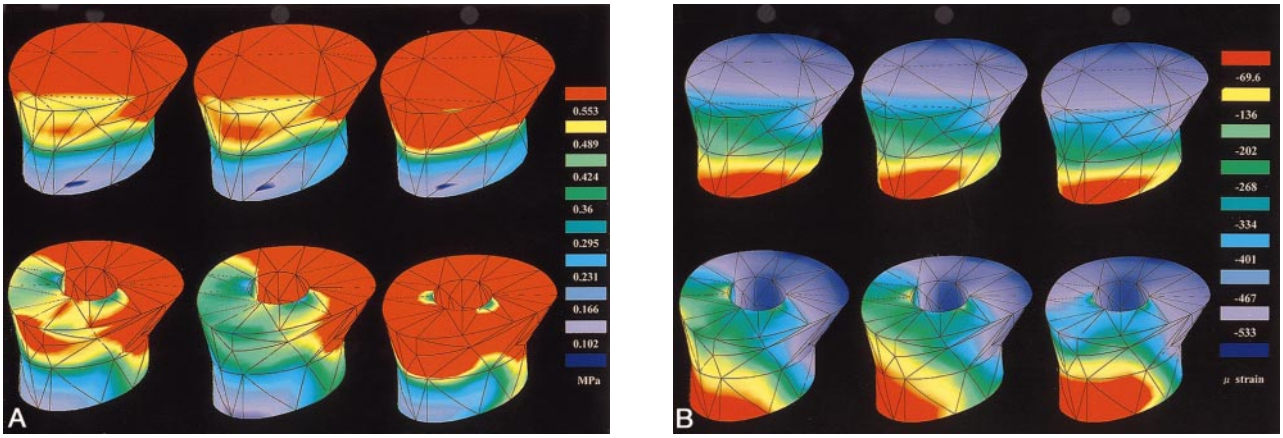

Fig. 4. The stress pattern, represented by the von Mises Stress (MPa) and the minimum principal strain pattern (μ strain) in the first cross-section of cancellous bone of the proximal femur before (top row) and after (bottom row) implantation. This figure shows (A) the stress pattern and (B) the strain pattern at first peak (P1; left column), valley (V; center column), and second peak (P2; right column).

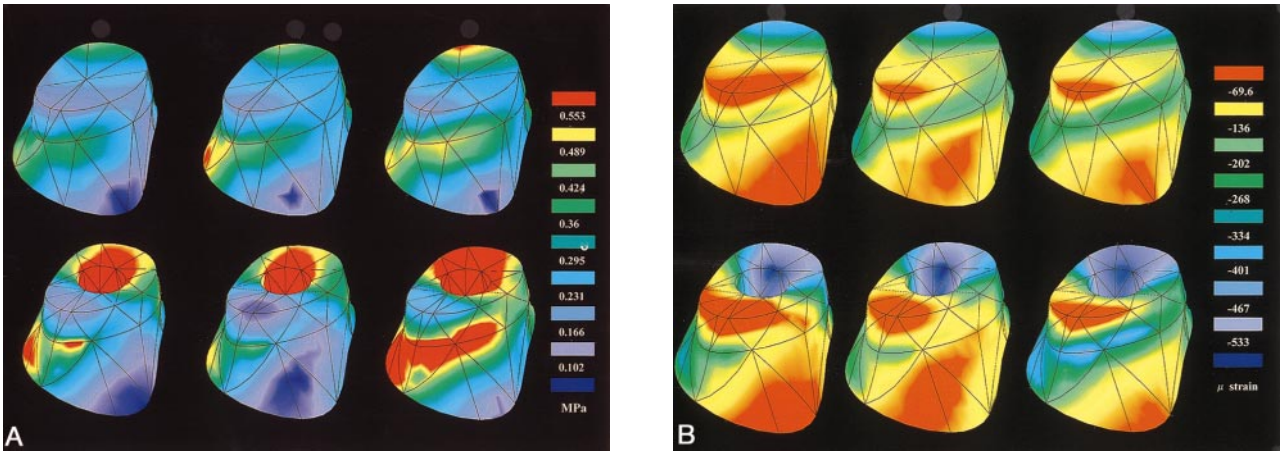

Fig. 5. The stress, represented by the von Mises Stress (MPa) and the minimum strain pattern (μ strain) in the second cross-section of cancellous bone of the proximal femur before (top row) and after (bottom row) implantation. The figure shows the (A) stress pattern and (B) strain pattern at first peak (P1; left column), valley (V; center column), and second peak (P2; right column).

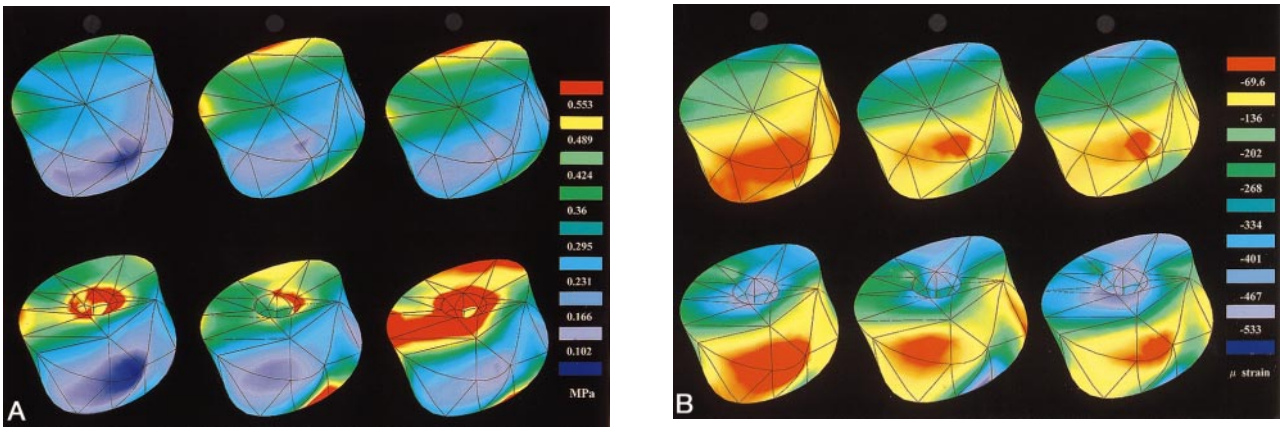

Fig. 6. The stress pattern, represented by the von Mises Stress (MPa) and the strain pattern (μ strain) in the third cross-section of cancellous bone of the proximal femur before (top row) and after (bottom row) implantation. This figure shows the (A) stress pattern and (B) strain pattern at first peak (P1; left column), valley (V; center column), and second peak (P2; right column).

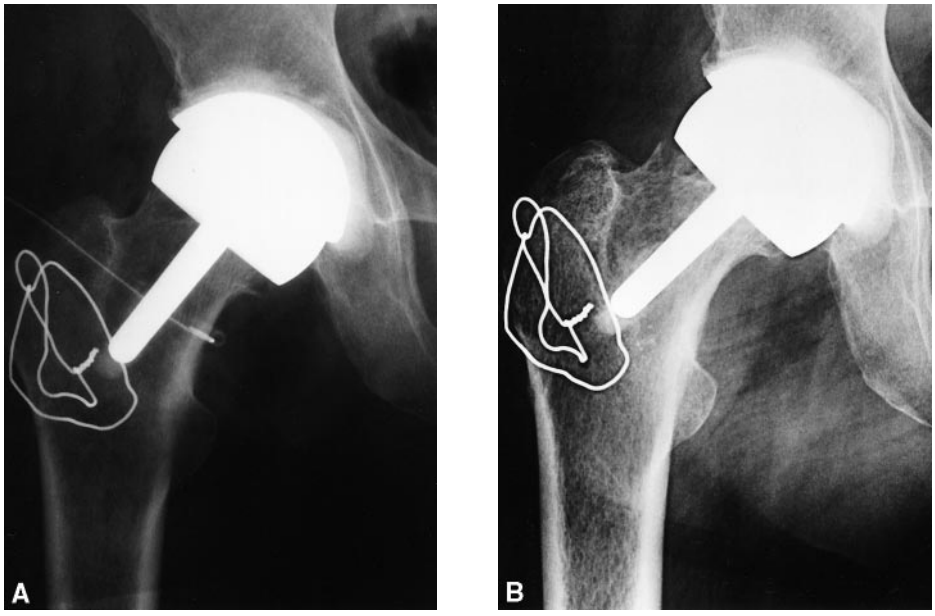

Fig. 7. (A) Preoperative and (B) 4-month postoperative radiographs of a 33-year-old woman with coxarthrosis due to adult-onset Still's disease who presented with a nontraumatic femoral neck fracture.

References

1. McMinn D, Treacy R, Lin K, et al: Metal on metal surface replacement of the hip. Clin Orthop 329S:89, 1996
2. Szivek JA, Gealer RL: Comparison of the deformation response of synthetic and cadaveric femora during simulated one-legged stance. J Appl Biomater 2:277, 1991
3. Szivek JA, Weng M, Karpman R: Variability in the torsional and bending response of a commercially available composite femur. J Appl Biomater 1:183, 1990
4. Szabo B, Babuska I: Finite element analysis. John Wiley & Sons, New York, 1991
5. Davy DT, Kotzar GM, Brown RH, et al: Telemetric force measurements across the hip after total arthroplasty. J Bone Joint Surg Am 70:45, 1988
6. Kotzer GM, Davy DT, Goldenberg VM, et al: Telemeterized in vivo hip joint force data: a report on two patients after total hip surgery. J Orthop Res 9:621, 1991
7. Crowninshield RD, Brand RA: A physiological based criterion of muscle force prediction in locomotion. J Biomech 14:793, 1981
8. Dostal WF, Andrews JG: A three-dimensional biomechanical model of hip musculature. J Biomech 14: 803, 1981
9. Huiskes R: The various stress pattern of press-fit, ingrown, and cemented femoral stems. Clin Orthop 261:27, 1990
10. Oomori H, Imamura S, Gesso H, et al: Biomechanical study of femoral stem load transfer in cementless total hip arthroplasty, using a nonlinear two-dimensional finite element method. p 239. In Imura S, Akamatsu N, Azuma H, Sawai K, and Tanaka S (eds): Hip biomechanics. Springer-Verlag, Tokyo, 1993
11. Marvin ES: Evolution and development of surface replacement arthroplasty. Orthop Clin North Am 13:667, 1982
12. Howie DW, Campbell D, Mcgee M, et al: Wagner resurfacing hip arthroplasty. J Bone Joint Surg Am 72:708, 1990
13. Bradley GW, Freeman MAR, Revell PA: Resurfacing arthroplasty. Clin Orthop 220:137, 1987
14. De Waal Malefijt MC, Huiskes R: A clinical, radiological and biomechanical study of the TARA hip prosthesis. Arch Orthop Trauma Surg 112:220, 1993
15. Howie DW, Cornish B, Vernon-Roberts B: Resurfacing hip arthroplasty. Clin Orthop 255:144, 1990
16. Huiskes R, Strens PHGE, Heck JV, et al: Interface stresses in the resurfaced hip. Acta Orthop Scand 56:474, 1985
17. Orr TE, Beaupré GS, Carter DR, et al: Computer predictions of bone remodeling around porous-coated implants. J Arthroplasty 5:191, 1990
18. Schmalzried TP, Fowble VA, Ure KJ, et al: Metal on metal surface replacement of the hip. Clin Orthop 329S:106, 1996
19. Wagner M, Wagner H: Preliminary results of uncemented metal on metal stemmed and resurfacing hip replacement arthroplasty. Clin Orthop 329S:78, 1996
20. Shybut GT, Askew MJ, Horii RY, et al: Theoretical and experimental studies of femoral stresses following surface replacement hip arthroplasty. p 192. In The hip. CV Mosby, St Louis, 1980
21. Skinner HB, Kilgus DJ, Keyak J, et al: Correlation of computed finite element stresses to bone density after remodeling around cementless femoral implants. Clin Orthop 305:178, 1994

22. Hayes WC, Bouxsein ML: Biomechanics of cortical and trabecular bone: implications for assessment of fracture risk. p 85. In Mow VC, Hayes WC (eds): Basic Orthopaedic Biomechanics. Lippincott-Raven, Philadelphia, 1997
23. Phillips TW, Johnston G, Wood P: Selection of animal model for resurfacing hip arthroplasty. J Arthroplasty 2:111, 1987
24. Nordin M, Frankel VH: Biomechanics of bone. p 3. In Nordin M, Frankel VH (eds): Basic biomechanics of the musculoskeletal system, 2nd ed. Lea & Febiger, Philadelphia, 1989